Rapid riparian ecosystem recovery in low-latitudinal North China following the end-Permian mass extinction

Wenwei Guo[1, 2], Li Tian[2*], Daoliang Chu[2], Wenchao Shu[2], Michael J. Benton[3], Jun Liu[4], Jinnan Tong[2]

[1]College of Culture and Tourism, Zhangzhou Institute of Technology, Zhangzhou 363000, People's Republic of China; [2]State Key Laboratory of Biogeology and Environmental Geology, China University of Geosciences, Wuhan, 430074, People's Republic of China; [3]School of Earth Sciences, University of Bristol, BS8 1RJ, UK; [4]Institute of Vertebrate Paleontology and Paleoanthropology, Chinese Academy of Sciences, Beijing 100044, People's Republic of China

***Author for Correspondence:** Li Tian, Email: tianlibgeg@cug.edu.cn

Abstract

The greatest mass extinction at the end of the Permian, ca. 252 million years ago, led to a tropical dead zone on land and sea. The speed of recovery of life has been debated, whether fast or slow, and terrestrial ecosystems are much less understood than marine. Here, we show fast reestablishment of riparian ecosystems in low-latitude North China as little as ~2 million years after the end-Permian mass extinction. The initial ichnoassemblages in shallow lacustrine and fluvial facies of late Smithian age are monospecific, devoid of infaunalization, with apparent size reduction. In the following Spathian, relatively complex, multi-level, structured riverain ecosystems had been rebuilt including medium-sized carnivores, plant stems, root traces, increased ichnological complexity, and significantly increased infaunalization. Specifically, burrowing behavior had re-emerged as a key life strategy not only to minimize stressful climatic conditions, but possibly to escape predation.

Introduction

The end-Permian mass extinction (EPME) is one of the most devastating bio-crises in the history of life and it destroyed both marine and terrestrial ecosystems (Wignall, 2015; Fan et al., 2020). A key feature of the EPME was the clearing of life from tropical ecosystems (e.g., Sun et al., 2012). Environmental extremes, especially lethal heat, largely flattened the tropical biodiversity peak, and marine animals were forced to migrate poleward or into deeper water (Liu et al., 2020; Song et al., 2020). Such effects were more brutal on land. A tropical “tetrapod gap”, spanning between 15°N and ~31°S, prevailed in the Early Triassic, or at particular intervals of intense global warming, even though the nature, temporal duration and spatial range of the Tropical Dead Zone (TDZ) remain

debated (Bernardi et al., 2018; Allen et al., 2020; Romano et al., 2020; Liu et al., 2022).

Long-term environmental perturbations after the EPME resulted in delayed recovery in the sea until the Middle Triassic (Chen and Benton, 2012), although several fast evolvers bounced back fast before being killed by further repeat hyperthermal events through the Early Triassic, as evidenced by the Guiyang Biota found ~1 million years (Myr) after the EPME (Dai et al., 2023). However, the post-extinction recovery on land has remained largely unclear. The taxonomic diversity of vertebrates may have re-flourished soon after the extinction in European Russia (Tverdokhlebov et al., 2003), but it apparently took longer, until the latest Early Triassic, in the Central European Basin (e.g., Scholze et al., 2017; Mujal et al., 2025). Model results of tetrapod-dominated paleocommunities from the Karoo also displayed a short lived, unstable ecosystem during the Early Triassic *Lystrosaurus* Assemblage Zone, before being replaced by a globally stable ecological structure established in the Middle Triassic (Roopnarine et al., 2019; Viglietti et al., 2022). It seemed that plants showed a quick return in Australia (Vajda and Kear, 2024), yet reorganization of floral communities was hindered by repeated climatic stressors, such as the Smithian–Spathian warming event (Mays et al., 2020; Vajda et al., 2020). Likewise, the initial construction of the mesophytic flora was in the earliest Middle Triassic in North China (Shu et al., 2022).

Other body fossils, especially non-marine invertebrates, are relatively scarce in the post-extinction interval. The earliest Middle Triassic riverine community, consisting of insects, rare fishes and trace fossils in equatorial western peri-Tethys (Baucon et al., 2014; Mujal et al., 2017; Matamales-Andreu et al., 2021) and the Anisian–Ladinian deep lake biota, comprising diverse insects, fishes, fish coprolites and plants in tropical North China (Zhao et al., 2020), were thought to be representative of recovered tropical terrestrial ecosystems after the EPME. However, recent

studies have revealed that biodiversity was not as low as expected in North China from the ichnological point of view, because relatively diverse trace fossils have been found in upper Lower Triassic deposits with moderate bioturbation (Guo et al., 2019; Xing et al., 2021; Zheng et al., 2021). Here, we report an unexpectedly rapidly recovered ecosystem from the TDZ after the EPME, based on compiled data of vertebrates, invertebrate trace fossils, and plant remains from Lower Triassic successions and outcrops in North China, to show how animals survived in harsh conditions and how the ecosystems finally recovered from the mass extinction event.

Geological Settings and Methods

Abundant trace fossils have been identified from the uppermost Permian–Lower Triassic of the Shichuanhe, Dayulin, Liulin sections and Hongyatou, Tuncun, Mafang outcrops in the Central North China Basin (Fig. 1). During the early Mesozoic, the North China Block was located at about 20°N based on paleomagnetic reconstruction (Huang et al., 2018; Guo et al., 2022). The Permo-Triassic strata, typically terrestrial red-beds, comprising the Sunjiagou, Liujiagou, Heshanggou (HSG) and Ermaying formations in ascending order, display varied depositional environments from fluvial to lacustrine facies (See Figure S1 and Table S1 in the Supporting Information). The Sunjiagou Formation mainly consists of red massive siltstone and intercalated sandstone of varied thickness, and paleosols and trace fossils were locally developed, demonstrating floodplain to lakeshore facies (Ji et al., 2022; Yu et al., 2022). The Liujiagou Formation is characterized by thick cross-bedded sandstones and intraclast conglomerates. Lenticular sand bodies and erosive bases of sandstones are common in the lower part, indicating fluvial channel facies under braided river systems (Zhu et al., 2019; Ji et al., 2022). Interlayered thick siltstones of lakeshore facies increase upwards, accompanied

by weak evidence of biological activity. The HSG is dominated by massive siltstones, with multi-layered paleosols, diverse trace fossils and some plant remains, belonging to alluvial plain and lakeshore facies, with periodic aerial exposure (Zhu et al., 2020; Ji et al., 2022).

Recently, a U-Pb CA-ID-TIMS age calibrated magnetostratigraphy from the Shichuanhe section provided a basic geochronological timescale for the fossil-poor strata in North China (Guo et al., 2022; Figure S2). Accordingly, the Permian–Triassic Boundary is constrained in the upper part of the Sunjiagou Formation based on the age of 252.21 ± 0.15 million years ago (Ma), with the base of the Smithian and Spathian being roughly located in the lower and upper Liujiagou Formation respectively. However, loss of several magnetozones in a regional hiatus makes it difficult to place the Lower–Middle Triassic Boundary precisely, which was tentatively put at the lithological contact of the HSG and the overlying Ermaying Formation (Guo et al., 2022). The 245–247 Ma ages from tuff layers at the base of the Ermaying Formation roughly support this correlation (Zhu et al., 2022).

In order to discriminate the recovery stages, several ichno-ecological criteria are used. Both bioturbation index (BI) and ichnofabric index (ii), which have been critically reviewed by Luo et al. (2020), are used to quantify bioturbation intensity. Values of ii and BI, ranging from 1–6 and 0–6, respectively, co-indicate the gradual increase of biotic disturbance from no bioturbation to total homogenization of sediments. Ichnodiversity represents the number of ichnotaxa, but it is not strictly equivalent to biodiversity, as a certain trace can be made by different animals and multiple trace types can originate from a single taxon (Luo et al., 2019). Ichnodisparity emphasizes the variability of architectural designs of trace fossils (Buatois et al., 2017), morphiologically distinct forms being termed ichnomorphs. Therefore, both ichnodiversity and ichnodisparity are employed to assess the behavioral responses of animals and the stage of infaunal biotic recovery (Table S2–4). Size and

penetration depth are also measured in places that can represent the average level of each burrow. Tiering, referring to the life position of an animal vertically in the sediment, is divided into surficial, semi-infaunal (0–0.5 cm), shallow (0.5–6 cm), intermediate (6–12 cm) and deep infaunal tiers (> 12 cm), based on Minter et al. (2017).

Thin sections of plant stem specimens were prepared to examine vertical and cross-sectional microstructures. Meanwhile, Micro-CT scanning (SkyScan 1172 X-ray; State Key Laboratory of Biogeology and Environmental Geology) was employed to reconstruct the internal structures of stems.

Results and Discussion

Infaunal Crisis and Living Strategy after the EPME in North China

An infaunal crisis, marked by the disappearance of the moderately diversified pre-extinction ichnofauna and the absence of biogenic structures, is identified in successions of late Changhsingian–early Smithian age. The latest Permian floodplain facies were mainly occupied by shallow–intermediate tiers of freely motile non-specialized deposit-feeding animals (Figure 1), akin to the Paleozoic suites reported before (Minter et al., 2017). Both ichnodiversity and ichnodisparity decline abruptly in the middle Sunjiagou Formation (near the 252.21 Ma aged tuff layer), following a prolonged non-bioturbated interval (Guo et al., 2019, 2022; Xing et al., 2021). The infaunal crisis was contemporary with the extirpation of the pareiasaur fauna (*Shihtienfenia*) and deforestation of the youngest Palaeozoic *Ullmannia-Pseudovoltzia-Germaropteris* assemblage in North China, representing the EPME on land (Liu et al., 2022; Shu et al., 2022).

The early recovery ichnofauna preserved in the upper Liujiagou Formation, about late Smithian

in age, was short-lived. This lakeshore ichnofauna, including seven ichnogenera of six ichnomorphs, is characterized by surficial and semi-infaunal tiered simple burrows or trails, with rare trackways and root traces, which weakly disturbed the sediments (Figure S3). Dwarfism in trace makers is observed from all ichnogenera, with burrow sizes reduced from a mean of 4.06 mm before the EPME (n = 779) to 2.06 mm (n = 341) in the late Smithian (Figure 4 and Figure S7), and as seen in individual ichnogenera such as *Kouphichnium* (Shu et al., 2018). The depauperate ichnofauna of the late Smithian was monospecific, representing initial recolonization of empty niches by opportunists. However, recurrent occurrences of microbially induced sedimentary structures (MISS) in the Liujiagou Formation show that depressed ecosystems persisted into the Smithian (Tu et al., 2016; Chu et al., 2017). Earlier work has shown that increases in microbial abundance were generally associated with hyperthermal events, the principal cause for mass extinction on land (Mays et al., 2021). Accumulations of microbes were favored by low dissolved oxygen concentration conditions and their secondary metabolites could also be toxic to animals (Pacton et al., 2011; Paerl and Otten, 2013). Therefore, repeated thriving of MISS during the Dienerian–Smithian interval disrupted ecological stability in freshwater ecosystems and delayed biotic recovery.

Abundant trace fossils are identified in the Spathian HSG Formation, comprising 16 ichnogenera of nine ichnomorphs, and two informally designated types (Figure 2 and Figure S4□5). This morphologically complex ichnofauna was dominated by actively filled burrows, with few arthropod trackways, which were probably produced by decapod crustaceans, myriapods and insects (Table S5). The lakeshore and alluvial plain facies were occupied by multi-tiered traces, including surficial trackways (e.g., *Diplichnites*; *Kouphichnium*), semi-infaunal (e.g., *Helminthoidichnites*; *Gordia*), shallow (e.g., *Palaeophycus*; *Scoyenia*), intermediate (e.g., *Taenidium*) and deep tiers

(*Camborygma*; *Skolithos*; Figure 1c). Trace producers that colonized varied ecospace and shallower tiers are generally crosscut by deeper penetrative burrows (Figure 2a), resulting in moderately to substantially bioturbated deposits, with ii 2–3 and BI 3–4 at most layers. In several horizons, the uppermost few centimeters of sediments are totally obliterated, mostly by the activity of deposit feeding animals. However, distal terminal fan facies are weakly reworked by simple traces such as *Skolithos* and *Palaeophycus* or root traces. Additionally, average burrow sizes of all ichnogenera also increased to 3.9 mm in the HSG (n = 2241, Figure 4 and Figure S7–8).

Several large burrows in the Spathian indicate the occurrence of advanced ecosystem engineers. *Camborygma litonomos* were found in the basal HSG of the Shichuanhe section and outcrop in Hongyatou, co-occurring with *in situ* preserved *Neocalamites* plant fossils, and other traces, such as *Diplichnites*, *Monomorphichnus* and *Skolithos* (Figure S6). Surfaces of *C. litonomos* were occasionally intertwined with rhizotubules (Figure 2l), suggesting that those plants could be important constituents in the diet of crayfish or that the crayfish might have hidden among the roots. In addition, another large burrow was identified in the Liulin section; this sub-horizontal unbranched burrow displays probable longitudinal scratch marks on the external surface, but poor preservation and limited specimens hinder a definite designation (Figure S5). ?*Beaconites*, found in the lower part of the HSG at Mafang, are characterized by meniscate structures (Figure 2o–p and Figure S5C–E), akin to those of large *Beaconites* from breccia facies in the Devonian red sandstone of Britain (Brück, 1987). Although the biological nature of these large burrows cannot be confirmed, their activities increased biogenic reworking of sediment and soils, improved geochemical recycling and ecosystem complexity in the Spathian, implying key roles in ecosystem functioning.

Although climatic and environmental conditions in the early Spathian were still not cool and

wet enough for thriving and abundant life, a fossorial strategy would have been useful for terrestrial animals to avoid heat and aridity. Midday temperatures > 35□, as occurred during peaks of global warming at the EPME and at points through the Early Triassic, cannot be tolerated for long by terrestrial (or aquatic) animals (Benton, 2018; Liu et al., 2022). The increase in tetrapod burrow abundance and complexity in the Lower Triassic suggest that a fossorial lifestyle allowed tetrapods to endure harsh post-extinction environmental conditions (Marchetti et al., 2024). Likewise, we envisage that infaunalization could also have been a vital strategy for invertebrates to survive and thrive. More intensively occupied ecospace in the late Spathian, characterized by increased burrowing and complicated crosscutting relations among ichnogenera, may indicate an adaptive response to heightened predation pressure or competition for available resources.

Fast recovered terrestrial ecosystem in tropical region

Our results also shed light on the timing of the TDZ. The late Smithian-age ichnofauna, although impoverished, represents early opportunist-dominated communities that explore empty ecospace under inhospitable environments, which constrain persistence of the TDZ to the late Smithian in North China. Newly discovered tetrapods from the HSG provide crucial insights into Spathian aged ecosystems. Historically, vertebrates found in this lithological unit were exclusively from its middle–upper portions (Li et al., 2008; Figure 3-4). The presence of Archosauromorpha (e.g., *Fugusuchus*; Fig. 3c) and Procolophonomorpha (e.g., *Eumetabolodon*; Fig. 3d) could reflect their tolerance to hot and arid condition, while the initial diversification of archosauromorphs in the Olenekian was interpreted as a response to empty ecological space after the EPME (McLoughlin et al., 2020; Romano et al., 2020). Herein, a cluster of tetrapod skeletons, including a few articulated

bones, were found near the base of HSG (early Spathian; Figure 3i). Body trunk lengths are estimated at 30–40 cm for the vertebrates, and the postcranial skeleton suggests a carnivorous feeding strategy. Although the specimens are not yet fully prepared for taxonomic description, they clearly show the existence of tetrapods at this level, narrowing the "tetrapod gap" to the Spathian.

Plants, as key components of the ecosystem, were patchily distributed in the Early Triassic (Shu et al., 2022). However, root traces (rhizoliths) are quite abundant, especially in the Dayulin section (Figure 2d and Figure S6). The different styles of preservation and various morphologies of rhizoliths provide information about the moderately to relatively well-drained red paleosols in alluvial plain facies (Kraus and Hasiotis, 2006). Specifically, *in situ* preserved vertical *Neocalamites* stems and *Pleuromeia* found in the lower HSG of the Shichuanhe and Hongyatou sections both occur in tandem with crayfish trace fossils and other burrows.

Delayed terrestrial recovery was proposed based on the Tongchuan fauna from North China, which consisted of diverse insects, ostracods, fishes, etc, signalling a fully recovered deep lake ecosystem in the Middle Triassic, i.e., ~8–12 Myr after the EPME (Zheng et al., 2018; Zhao et al., 2020). However, compiled paleontological data herein show that ecosystems on land occurred in tropical regions as early as in the Spathian, ~2 Myr after the EPME (Figure S9). The enhanced floral coverage attributed to different types of roots and plant fossils had great impact on the initiation of a post-EPME ecosystem, especially the co-occurring stems and trace fossils, which suggest that riverain realms might have been refugia for the survival and evolution of the Spathian biota (Figure 5). Increased abundance and quantity of faunal communities can be inferred from ichnodiversity, with possible candidate trace-producers including limuloids, crayfishes, spinicaudatans, insects and even small-sized vertebrates (Table S5), and moderate bioturbation made by high-density resting

traces, respectively. Coeval tetrapods, despite being rare, do show the existence of carnivores and further complexity in local ecological structures. Reconstruction of freshwater ecosystems in the Spathian was also facilitated by amelioration of the climate (Figure 4). Paleosol-based paleoclimatic reconstructions suggest that precipitation was ~520–680 mm/y in the late Spathian, with pCO_2 estimated from paleosols at 1523 ± 417 ppm (Joachimski et al., 2022; Yu et al., 2022), indicating mitigation of hyperthermal conditions. Geochemical proxies of weathering intensity, salinity and clayiness, along with increased hygrophyte/xerophyte ratio, also demonstrate the transition to wetter conditions (Shu et al., 2022; Zhu et al., 2022).

Conclusions

The diverse community of the HSG Formation, consisting of tetrapods, plant stems, rhizoliths, and diverse ichnofossils suggests a rapid recovery of life in low-latitude terrestrial environments in the Spathian, as early as ~2 Myr after the end-Permian biotic crisis. The newly discovered vertebrate fossils are medium-sized carnivores of approximately early Spathian age, representing the earliest Triassic-aged tetrapods found in North China. High ichnodiversity and ichnodisparity, and three types of large burrows, not only result in intensified bioturbation, but provide additional information about the enriched local biota. Furthermore, enhanced burrowing behavior is considered a key survival-recovery strategy to adapt to harsh climatic and environmental conditions on land. The co-occurring trace fossils and stems, and coeval tetrapod in alluvial plain facies, suggest that the riverain regions could be refugia for the reorganization of post-EPME ecosystem.

Data Availability Statement

All supplementary data related to this paper is available in the end of this manuscript.

Article and author information

Author details

Wenwei Guo

- College of Culture and Tourism, Zhangzhou Institute of Technology, Zhangzhou, People's Republic of China
- State Key Laboratory of Biogeology and Environmental Geology, School of Earth Science, China University of Geosciences, Wuhan, People's Republic of China

Contribution: Conceptualization; Methodology; Validation; Formal analysis; Investigation; Data curation; Writing–original draft preparation; Writing–review & editing; Visualization

Competing interests: No competing interests declared

Li Tian

State Key Laboratory of Biogeology and Environmental Geology, School of Earth Science, China University of Geosciences, Wuhan, People's Republic of China

Contribution: Conceptualization; Methodology; Validation; Formal analysis; Investigation; Data curation; Writing–original draft preparation; Writing–review & editing; Visualisation; Project administration; Funding acquisition

For correspondence: tianlibgeg@cug.edu.cn

Competing interests: No competing interests declared

Daoliang Chu

State Key Laboratory of Biogeology and Environmental Geology, School of Earth Science, China University of Geosciences, Wuhan, People's Republic of China

Contribution: Conceptualization; Methodology; Validation; Investigation; Data curation; Writing–original draft preparation; Writing–review & editing; Visualization; Project administration; Funding acquisition

Competing interests: No competing interests declared

Wenchao Shu

State Key Laboratory of Biogeology and Environmental Geology, School of Earth Science, China University of Geosciences, Wuhan, People's Republic of China

Contribution: Methodology; Validation; Formal analysis; Investigation; Writing–original draft preparation; Writing–review & editing; visualization

Competing interests: No competing interests declared

Michael J. Benton

School of Earth Sciences, University of Bristol, UK

Contribution: Conceptualization; Methodology; Validation; Formal analysis; Investigation; Writing–review & editing; Visualization; Funding acquisition

Competing interests: No competing interests declared

Jun Liu

Institute of Vertebrate Paleontology and Paleoanthropology, Chinese Academy of Sciences, Beijing, People's Republic of China

Contribution: Conceptualization; Methodology; Validation; Formal analysis; Investigation; Writing–review & editing; Visualization; Funding acquisition

Competing interests: No competing interests declared

Jinnan Tong

State Key Laboratory of Biogeology and Environmental Geology, School of Earth Science, China University of Geosciences, Wuhan, People's Republic of China

Contribution: Conceptualization; Validation; Formal analysis; Investigation; Writing–review & editing; Visualization; Supervision; Project administration; Funding acquisition

Competing interests: No competing interests declared

Acknowledgments

We thank Kaixuan Ji, Gan Liu and Yuyang Wu for assistance in the field. We also thank anonymous reviewers for their comments and constructive suggestions. This work was supported by the National Natural Science Foundation of China (grant nos. 42030513) to L. T., D. C. and J. T., the Strategic Priority Research Program of the Chinese Academy of Sciences (grant no. XDB26000000) to J. L. and the Natural Environment Research Council (UK) of grant no. NE/P013724/1 to M. J. B.

References

Allen BJ, Wignall PB, Hill DJ, Saupe EE, Dunhill AM. 2020. The latitudinal diversity gradient of

tetrapods across the Permo-Triassic mass extinction and recovery interval. *Proceedings of the Royal Society B*, **287**: 20201125. https://doi.org/10.1098/rspb.2020.1125

Baucon A, Ronchi A, Felletti F, Neto de Carvalho C. 2014. Evolution of crustaceans at the edge of the end-Permian crisis: Ichnonetwork analysis of the fluvial succession of Nurra (Permian–Triassic, Sardinia, Italy). *Palaeogeography, Palaeoclimatology, Palaeoecology*, **410**: 74–103. https://doi.org/10.1016/j.palaeo.2014.05.034

Benton MJ. 2018. Hyperthermal-driven mass extinctions: killing models during the Permian–Triassic mass extinction. *Philosophical Transactions of the Royal Society A*, **376**: 20170076. https://doi.org/10.1098/rsta.2017.0076

Bernardi M, Petti FM, Benton MJ. 2018. Tetrapod distribution and temperature rise during the Permian-Triassic mass extinction. *Proceedings of the Royal Society B*, **285**: 20172331. https://doi.org/10.1098/rspb.2017.2331

Brück PM. 1987. A note on the trace fossil *Beaconites barretti* in the Old Red Sandstone of County Dublin, Ireland. *Proceedings of the Geologists' Association*, **98**: 259–263. https://doi.org/10.1016/S0016-7878(87)80043-3

Buatois LA, Wisshak M, Wilson MA, Mángano MG, 2017. Categories of architectural designs in trace fossils: a measure of ichnodisparity. *Earth-Science Reviews*, **164**: 102–181. https://doi.org/10.1016/j.earscirev.2016.08.009

Buatois LA, Borruel-Abadía V, De la Horra R, Galán-Abellán AB, López-Gómez J, Barrenechea JF, Arche A. 2021. Impact of Permian mass extinctions on continental invertebrate infauna. *Terra Nova*, **33**: 455–464. https://doi.org/10.1111/ter.12530.

Chen ZQ, Benton MJ. 2012. The timing and pattern of biotic recovery following the end-Permian

mass extinction. *Nature Geoscience*, **5**: 375–383. https://doi.org/10.1038/ngeo1475

Chu DL, Tong JN, Bottjer DJ, Song HJ, Song HY, Benton MJ, Tian Li, Guo WW. 2017. Microbial mats in the terrestrial Lower Triassic of North China and implications for the Permian–Triassic mass extinction. *Palaeogeography, Palaeoclimatology, Palaeoecology*, **474**: 214–231. https://doi.org/10.1016/j.palaeo.2016.06.013

Dai X, Davies JHFL, Yuan Z, Brayard A, Ovtcharova M, Xu GH, Liu XK, Smith CPA, Schweitzer CE, Li MT, Perrot MG, Jiang SY, Miao LY, Cao YR, Yan J, Bai RY, Wang FY, Guo W, Song HY, Tian L, Dal Corso J, Liu YT, Chu DL, Song HJ. 2023. A Mesozoic fossil lagerstätte from 250.8 million years ago shows a modern-type marine ecosystem. *Science*, **379**: 567–572. DOI: 10.1126/science.adf1622

Fan JX, Shen SZ, Erwin DH, Sadler PM, MacLeod N, Cheng QM, Hou XD, Yang J, Wang XD, Wang Y, Zhang H, Chen X, Li GX, Zhang YC, Shi YK, Yuan DX, Chen Q, Zhang LN, Li C, Zhao YY. 2020. A high-resolution summary of Cambrian to early Triassic marine invertebrate biodiversity. *Science*, **367**: 272–277. DOI: 10.1126/science.aax4953

Guo WW, Tong JN, Tian L, Chu DL, Bottjer DJ, Shu WC, Ji KX. 2019. Secular variations of ichnofossils from the terrestrial Late Permian-Middle Triassic succession at the Shichuanhe section in Shaanxi Province, North China. *Global and Planetary Change*, **181**: 102978. https://doi.org/10.1016/j.gloplacha.2019.102978

Guo WW, Tong JN, He Q, Hounslow MW, Song HY, Dal Corso J, Wignall PB, Ramezani J, Tian L, Chu DL. 2022. Late Permian–Middle Triassic magnetostratigraphy in North China and its implications for terrestrial-marine correlations. *Earth and Planetary Science Letters*, **585**: 117519. https://doi.org/10.1016/j.epsl.2022.117519

Huang BC, Yan Y, Piper JDA, Zhang D, Yi Z, Yu S, Zhou T. 2018. Paleomagnetic constraints on the paleogeography of the East Asian blocks during Late Paleozoic and Early Mesozoic times. *Earth-Science Reviews*, **186**: 8–36. https://doi.org/10.1016/j.earscirev.2018.02.004

Ji K, Wignall PB, Tong JN, Yu YY, Guo WW, Shu WC, Chu DL. 2022. Sedimentology of the latest Permian to Early Triassic in the terrestrial settings of the North China Basin: Low-latitude climate change during a warming-driven crisis. *Geological Society of America Bulletin*, **135**: 481-503. https://doi.org/10.1130/b36260.1

Joachimski MM, Müller J, Gallagher TM, Mathes G, Chu DL, Mouraviev F, Silantiev V, Sun YD, Tong JN. 2022. Five million years of high atmospheric CO_2 in the aftermath of the Permian-Triassic mass extinction. *Geology*, **50**: 650–654. https://doi.org/10.1130/G49714.1

Kraus MJ, Hasiotis ST. 2006. Significance of different modes of rhizolith preservation to interpreting paleoenvironmental and paleohydrologic settings: Examples from Paleogene paleosols, Bighorn Basin, Wyoming, U.S.A. *Journal of Sedimentary Research*, **76**: 633–646. https://doi.org/10.2110/jsr.2006.052

Li JL, Wu X, Zhang F. 2008. *The Chinese Fossil Reptiles and Their Kin*. Science Press, Beijing.

Liu J, Abdala F, Angielczyk KD, Sidor CA. 2022. Tetrapod turnover during the Permo-Triassic transition explained by temperature change. *Earth-Science Reviews*, **224**: 103886. https://doi.org/10.1016/j.earscirev.2021.103886.

Liu XK, Song HJ, Bond DPG, Tong JN, Benton MJ. 2020. Migration controls extinction and survival patterns of foraminifers during the Permian-Triassic crisis in South China. *Earth-Science Reviews*, **209**: 103329. https://doi.org/10.1016/j.earscirev.2020.103329

Luo M, Shi GR, Buatois LA, Chen ZQ. 2020. Trace fossils as proxy for biotic recovery after the

end-Permian mass extinction. A critical review. *Earth-Science Reviews*, **203**: 103059. https://doi.org/10.1016/j.earscirev.2019.103059

Matamales-Andreu R, Penalver E, Mujal E, Oms O, Scholze F, Juarez J, Galobart A, Fortuny J. 2021. Early-Middle Triassic fluvial ecosystems of Mallorca (Balearic Islands): Biotic communities and environmental evolution in the equatorial western peri-Tethys. *Earth-Science Reviews*, **222**: 103783. https://doi.org/10.1016/j.earscirev.2021.103783

Marchetti L, MacDougall MJ, Buchwitz M, Canoville A, Herde M, Kammerer CF, Fröbisch J. 2024. Origin and early evolution of vertebrate burrowing behaviour. *Earth-Science Reviews*, **250**: 104702. https://doi.org/10.1016/j.earscirev.2024.104702

Mays C, Vajda V, Frank TD, Fielding CR, Nicoll RS, Tevyaw AP, McLoughlin S. 2020. Refined Permian–Triassic floristic timeline reveals early collapse and delayed recovery of south polar terrestrial ecosystems. *Geological Society of America Bulletin*, **132**: 1489–1513. https://doi.org/10.1130/B35355.1

Mays C, McLoughlin S, Frank TD, Fielding CR, Slater SM, Vajda V. 2021. Lethal microbial blooms delayed freshwater ecosystem recovery following the end-Permian extinction. *Nature Communications*, **12**: 5511. https://doi.org/10.1038/s41467-021-25711-3

McLoughlin S, Mays C, Vajda V, Bocking M, Frank TD, Fielding CR. 2020. Dwelling in the dead zone—Vertebrate burrows immediately succeeding the end-Permian extinction event in Australia. *Palaios*, **35**: 342-357. https://doi.org/10.2110/palo.2020.007

Minter NJ, Buatois LA, Mángano MG, Davies NS, Gibling MR, MacNaughton RB, Labandeira CC. 2017. Early bursts of diversification defined the faunal colonization of land. *Nature Ecology & Evolution*, **1**: https://doi.org/10.1038/s41559-017-0175

Mujal E, Fortuny J, Bolet A, Oms O, López JÁ. 2017. An archosauromorph dominated ichnoassemblage in fluvial settings from the late Early Triassic of the Catalan Pyrenees (NE Iberian Peninsula). *PLoS One*, **12** (4): e0174693. http://dx.doi.org/10.1371/journal.pone.0174693

Mujal E, Sues HD, Moreno R, Moreno R, Schaeffer J, Sobral G, Chakravorti S, Spiekman SNF, Schoch RR. 2025. Triassic terrestrial tetrapod faunas of the Central European Basin, their stratigraphical distribution, and their palaeoenvironments. Earth-Science Reviews, 105085.

Pacton M, Gorin GE, Vasconcelos C. 2011. Amorphous organic matter—Experimental data on formation and the role of microbes. *Review of Palaeobotany and Palynology*, **166**: 253–267. https://doi.org/10.1016/j.revpalbo.2011.05.011

Paerl HW, Otten TG. 2013. Harmful cyanobacterial blooms: causes, consequences, and controls. *Microbial Ecology*, **65**: 995–1010. https://doi.org/10.1007/s00248-012-0159-y

Romano M, Bernardi M, Petti FM, Rubidge B, Hancox J, Benton MJ. 2020. Early Triassic terrestrial tetrapod fauna: a review. *Earth-Science Reviews*, **210**: 103331. https://doi.org/10.1016/j.earscirev.2020.103331

Roopnarine PD, Angielczyk KD, Weik A, Dineen A. 2019. Ecological persistence, incumbency and reorganization in the Karoo Basin during the Permian-Triassic transition. *Earth-Science Reviews*, **189**: 244−263. https://doi.org/10.1016/j.earscirev.2018.10.014

Scholze F, Wang Z, Kirscher U, Kraft J, Schneider JW, Götz AE, Joachimski MM, Bachtadse V. 2017. A multistratigraphic approach to pinpoint the Permian-Triassic boundary in continental deposits: the Zechstein–Lower Buntsandstein transition in Germany. Global and Planetary Change, **152**: 129–151. http://dx.doi.org/10.1016/j.gloplacha.2017.03.004

Shu WC, Tong JN, Tian L, Benton MJ, Chu DL, Yu JX, Guo WW. 2018. Limuloid trackways from Permian–Triassic continental successions of North China. *Palaeogeography, Palaeoclimatology, Palaeoecology*, **508**: 71–90. https://doi.org/10.1016/j.palaeo.2018.07.022

Shu WC, Tong JN, Yu JX, Hilton J, Benton MJ, Shi X, Diez JB, Wignall PB, Chu DL, Tian L, Yi, ZX, Mao YD. 2022. Permian−Middle Triassic floral succession in North China and implications for the great transition of continental ecosystems. *Geological Society of America Bulletin*, **135**: 1747–1767. https://doi.org/10.1130/B36316.1

Song HJ, Huang S, Jia EH, Dai X, Wignall PB, Dunhill AM. 2020. Flat latitudinal diversity gradient caused by the Permian-Triassic mass extinction. *Proceedings of the National Academy of Sciences of the United States of America*, **117**: 17578–17583. https://doi.org/10.1073/pnas.1918953117

Sun YD, Joachimski MM, Wignall PB, Yan CB, Chen YL, Jiang HS, Wang LN, Lai XL. 2012. Lethally hot temperatures during the Early Triassic greenhouse. *Science*, **338**: 366–370. DOI:10.1126/science.1224126

Tu CY, Chen ZQ, Retallack GJ, Huang Y, Fang Y. 2016. Proliferation of MISS-related microbial mats following the end-Permian mass extinction in terrestrial ecosystems: Evidence from the Lower Triassic of the Yiyang area, Henan Province, North China. *Sedimentary Geology*, **333**: 50−69. https://doi.org/10.1016/j.sedgeo.2015.12.006

Tverdokhlebov VP, Tverdokhlebova GI, Surkov MV, Benton MJ. 2003. Tetrapod localities from the Triassic of the SE of European Russia. *Earth-Science Reviews*, **60**: 1–66. https://doi.org/10.1016/S0012-8252(02)00076-4

Vajda V, McLoughlin S, Mays C, Frank TD, Fielding CR, Tevyaw A, Lehsten V, Bocking M, Nicoll

RS. 2020. End-Permian (252 Mya) deforestation, wildfires and flooding – an ancient biotic crisis with lessons for the present. *Earth and Planetary Science Letters*, **529**: 115875. https://doi.org/10.1016/j.epsl.2019.115875

Vajda V, Kear BP. 2024. An earliest Triassic riparian ecosystem from the Bulgo Sandstone (Sydney Basin), Australia: palynofloral evidence of a high-latitude terrestrial vertebrate habitat after the end-Permian mass extinction. *Alcheringa: An Austalasian Journal of Palaeontology*, 1−12. https://doi.org/10.1080/03115518.2024.2392489

Viglietti PA, Rojas A, Rosvall M, Klimes B, Angielczyk KD. 2022. Network-based biostratigraphy for the late Permian to mid-Triassic Beaufort Group (Karoo Supergroup) in South Africa enhances biozone applicability and stratigraphic correlation. *Palaeontology*, **65**: e12622. https://doi.org/10.1111/pala.12622

Wignall PB. 2015. *The Worst of Times: How Life on Earth Survived Eighty Million Years of Extinction*. Princeton University Press, NJ: Princeton.

Xing ZF, Lin J, Fu YX, Zheng W, Liu YL, Qi YA. 2021. Trace fossils from the Lower Triassic of North China — a potential signature of the gradual recovery of a terrestrial ecosystem. *Palaeoworld*, **30**: 95–105. https://doi.org/10.1016/j.palwor.2020.06.002

Yu YY, Tian L, Chu DL, Song HY, Guo WW, Tong JN. 2022. Latest Permian–Early Triassic paleoclimatic reconstruction by sedimentary and isotopic analyses of paleosols from the Shichuanhe section in central North China Basin. *Palaeogeography, Palaeoclimatology, Palaeoecology*, **585**: 110726. https://doi.org/10.1016/j.palaeo.2021.110726

Zhao XD, Zheng DR, Xie GW, Jenkyns HC, Guan CG, Fang Y, He J, Yuan XQ, Xue NH, Wang H, Li S, Jarzembowski, EA, Zhang HC, Wang B. 2020. Recovery of lacustrine ecosystems after the

end-Permian mass extinction. *Geology*, **48**: 609–613. https://doi.org/10.1130/G47502.1

Zheng DR, Chang SC, Wang H, Fang Y, Wang J, Feng CQ, Xie GW, Jarzembowski EA, Zhang HC, Wang B. 2018. Middle-Late Triassic insect radiation revealed by diverse fossils and isotopic ages from China. *Science Advances*, **4**: eaat1380. https://doi.org/10.1126/sciadv.aat1380

Zheng W, Wan EZ, Xu X, Li D, Dai MY, Qi YA, Xing ZF, Liu YL. 2021. The variations of terrestrial trace fossils and sedimentary substrates after the end-Permian extinction in the Dengfeng area, North China. *Geological Journal*, **58**: 1223–1238. https://doi.org/10.1002/gj.4657

Zhu ZC, Liu YQ, Kuang HW, Benton MJ, Newell AJ, Xu H, An W, Ji SA, Xu SC, Peng N, Zhai QG. 2019. Altered fluvial patterns in North China indicate rapid climate change linked to the Permian-Triassic mass extinction. *Scientific Reports*, **9**: 16818. https://doi.org/10.1038/s41598-019-53321-z

Zhu ZC, Kuang HW, Liu YQ, Benton MJ, Newell AJ, Xu H, An W, Ji SA, Xu SC, Peng N, Zhai QG. 2020. Intensifying aeolian activity following the end□Permian mass extinction: Evidence from the Late Permian–Early Triassic terrestrial sedimentary record of the Ordos Basin, North China. *Sedimentology*, **67**: 2691-2720. https://doi.org/10.1111/sed.12716

Zhu ZC, Liu YQ, Kuang HW, Newell AJ, Peng N, Cui MM, Benton MJ. 2022. Improving paleoenvironment in North China aided Triassic biotic recovery on land following the end-Permian mass extinction. *Global and Planetary Change*, **216**: 103914. https://doi.org/10.1016/j.gloplacha.2022.103914

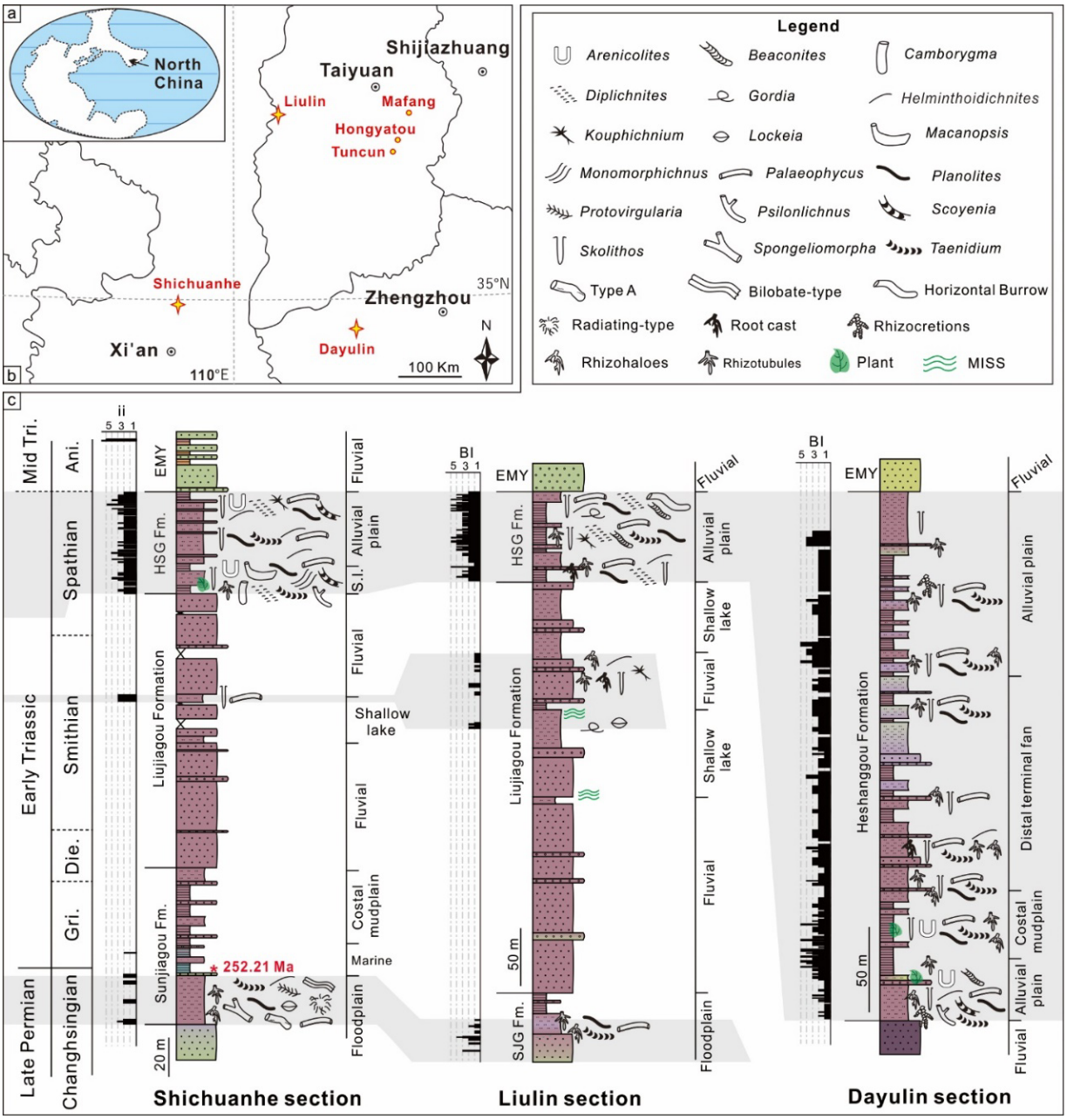

Figure 1. Location of the studied regions and lithological columns. (a–b) Permian-Triassic paleogeographic map of North China and the studied successions (stars) and outcrops (points). Base map is modified from Sun et al. (2012). (c) Depositional facies and detailed distribution of trace fossils in three main successions.

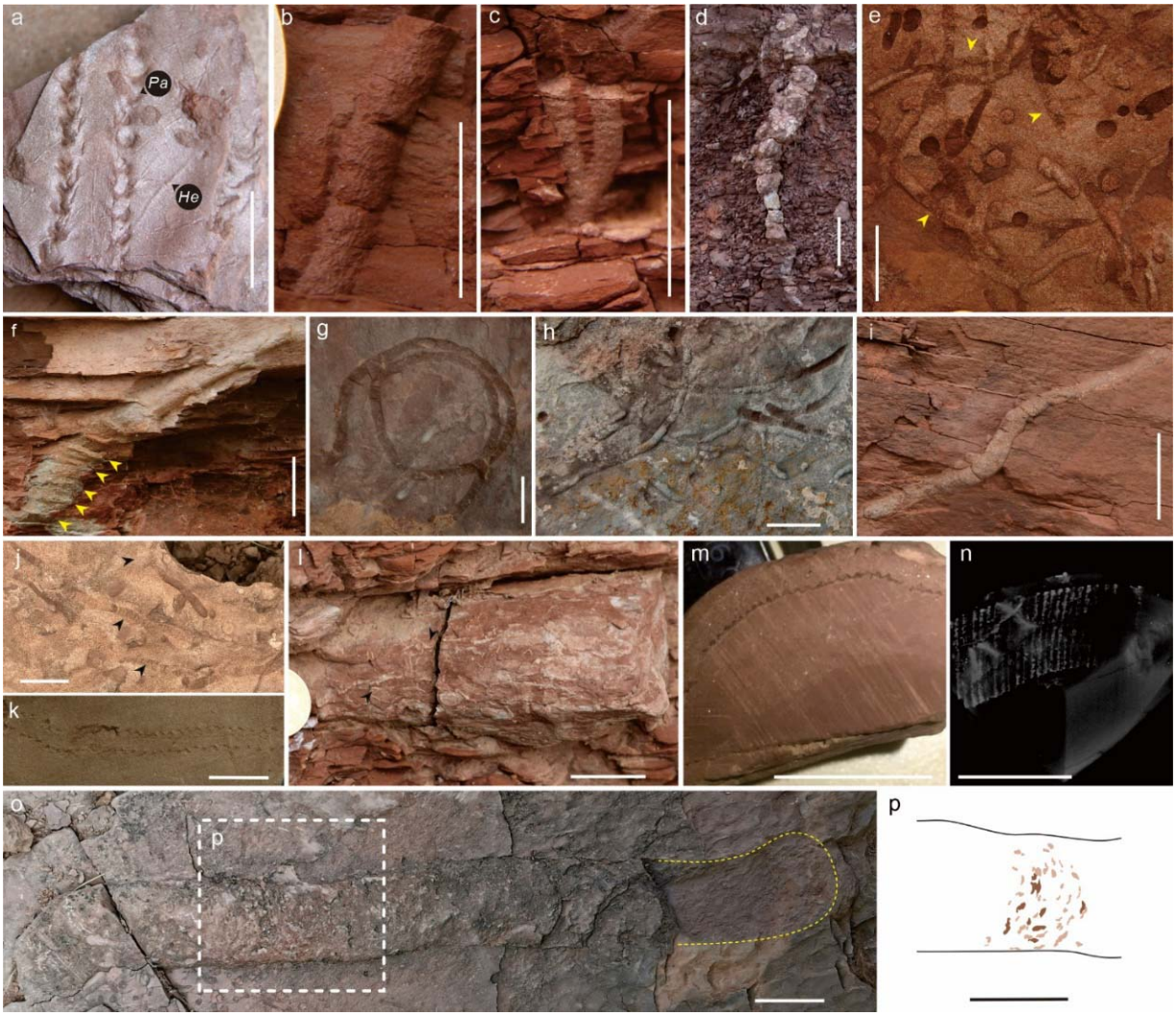

Figure 2. Ichnofossils from the Heshanggou Formation of North China. (a) Shallow tiers *Kouphichnium* and *Helminthoidichnites* (He) are crosscut by immediate tier *Palaeophycus* (Pa). (b) *Skolithos* cf. *serratus* with faint oblique striations. (c) Y-shaped *Psilonichnus* isp. (d) Downward unbranched and tapered rhizocretion. (e) Shallow tiers *Beaconites coronus*, arrows show tightly stacked arcuate meniscus. (f) *Camborygma* isp. shows enlarged terminal chamber and possible transverse scratches (arrows). (g) *Gordia* isp. with darker and finer infills. (h) High density *Palaeophycus tubularis* preserved on the sole of thick sandstone. (i) Inclined *Planolites beverleyensis* within siltstone. (j) *Taenidium barretti* (arrows) pass through the rippled surface. (k) Horizontal *Camborygma*, the outer surface is intertwined with tiny root traces (arrows). (l) Biserial

Diplichnites gouldi. (m–n) Internode cross-section of *Neocalamites* stem and micro-CT structure, showing the clear ribs and grooves. (o–p) Large ?*Beaconites* on top of rippled sandstone, rectangle in (p) shows meniscus-like portions comprising of gritty infillings. Scale bar of (d, f, h, o–p) are 40 mm, the rest are all 20 mm.

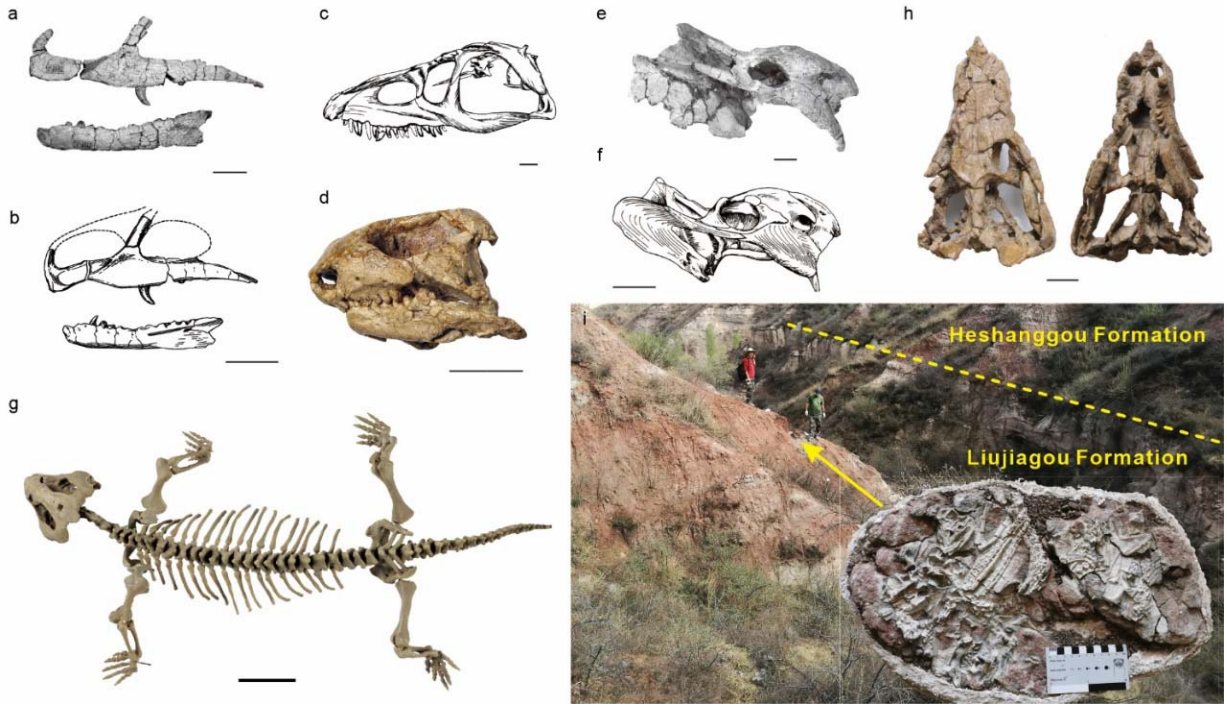

Figure 3. Vertebrates from the Heshanggou Formation of North China. (a–b) Skull elements of *Xilousuchus sapingensis* and drawings. (c) *Fugusuchus hejiapanensis*. (d) *Eumetabolodon bathycephalus*. (e–f) *Shaanbeikannemeyeria xilouensis* and drawing. (g) *Pentaedrusaurus ordosianus*. (h) *Hazhenia concava*, (i) Dashed line shows the boundary between the Liujiagou and Heshanggou formations. Arrow displays fossil horizon of the inserted picture at the base of the Heshanggou Formation. (b, c, f) are from Li et al. (2008). Scale bars are 40 mm.

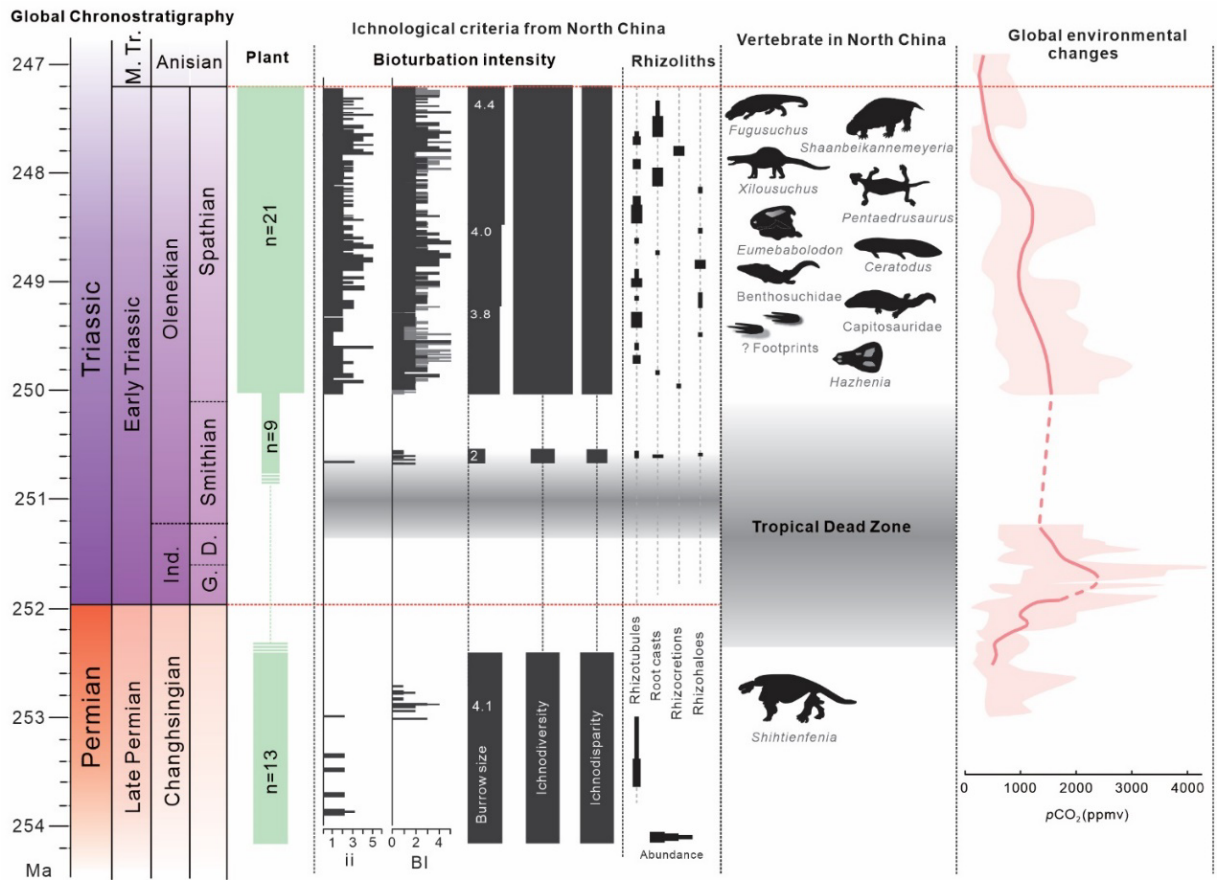

Figure 4. Ichnofossil data in North China and global terrestrial ecosystem changes from latest Permian to earliest Middle Triassic. Geochronological timescale is based on the latest version of the International Chronostratigraphic Chart (https://stratigraphy.org/). Plant richness from Shu et al. (2022). Numbers in Burrow size column represent the mean trace fossil sizes from the investigated interval. Drainage conditions of paleosols are inferred from preservation of rhizoliths and their relative depths. Ranges of microbially induced sedimentary structures (MISS) are from Chu et al. (2017). Atmospheric CO_2 curves are modified from Joachimski et al. (2022). Abbreviations: Ind. = Induan; G. = Griesbachian; D. = Dienerian.

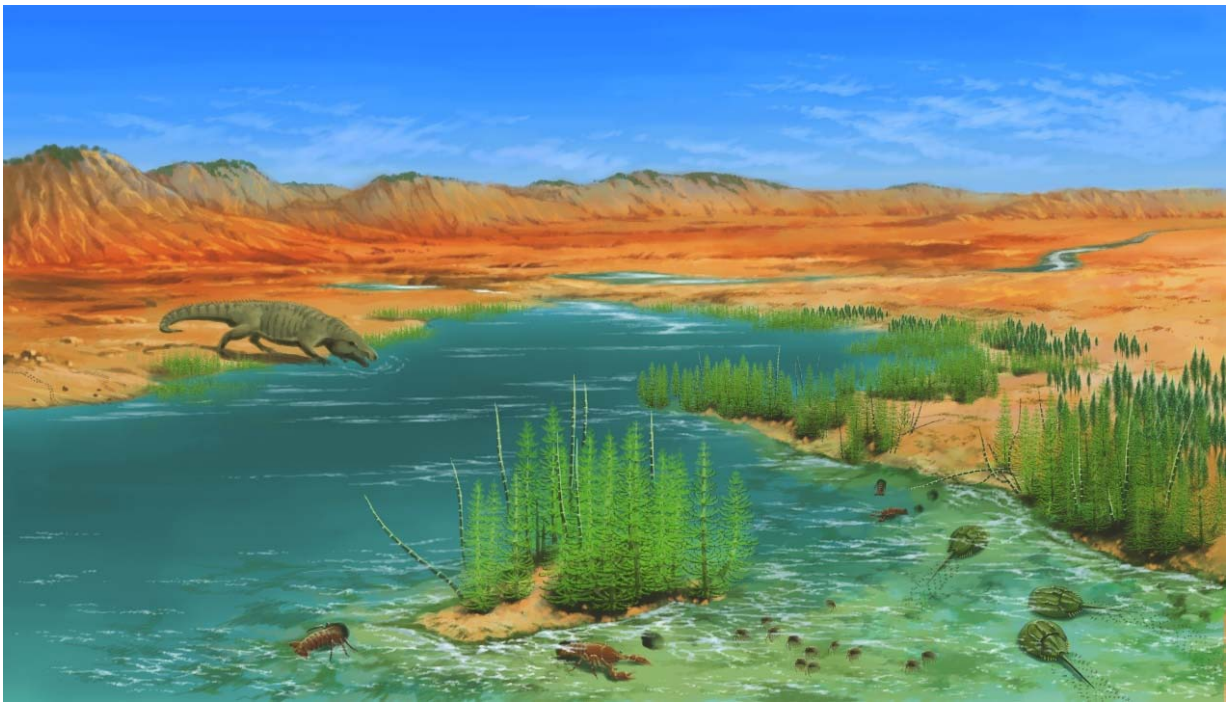

Figure 5. Reconstruction of the Spathian (Heshanggou Formation) coastal mudplain to alluvial ecosystem in North China. Plant communities in the coastal mudplain and alluvial facies are depauperate, dominated by *Neocalamites* and *Pleuromeia*, and only diverse at the top of the Heshanggou Formation (late Spathian; Shu et al., 2022). Fossil plants and tetrapods, coupled with diverse invertebrate, including limuloids, crayfish, spinicaudatans, and insects, etc., reveal reorganization of a relatively complex ecosystem in riverain regions during the Spathian. The artistic illustration was credited by J. Sun.